Observation of ferroelectric domains in bismuth ferrite using coherent diffraction techniques

James Vale

October 25, 2011

Abstract

Multiferroic materials have significant potential for both the scientific and industrial communities. Those which are both ferromagnetic and ferroelectric with a transition temperature greater than ambient are of particular interest. This paper details the use of coherent X-ray imaging techniques to obtain maps of ferroelectric domains in bismuth ferrite, $BiFeO_3$.

1 Introduction

Multiferroics have, especially in the past few years, been of great interest to the scientific community as these materials exhibit two of the following properties: ferroelectricity, ferromagnetism and ferroelasticity. For certain magnetic point groups, a curious effect can occur. If an electric field **E** is applied, a spontaneous magnetization can occur:

$$M_j = \alpha_{ij} E_i,$$

where α_{ij} is a tensor specific for each point group. Conversely a spontaneous polarization can occur when a magnetic field is applied:

$$P_i = \alpha_{ij} H_j.$$

This is known as the linear magnetoelectric effect. This effect has been earmarked by industry, where there is the potential to create solid-state memory devices which can be read magnetically and written to electrically.

However the magnetoelectric effect usually only occurs below a critical temperature. Currently there are very few materials for which the critical point is in the region of ambient temperature; many materials only exhibit multiferroicity below 100K. One material which has been studied extensively is bismuth ferrite, $BiFeO_3$, (space group *R3c*, Fig. 1) [1] which is an exception to the general trend. The critical temperature for the paraelectric/ferroelectric transition (Curie temperature) is $\sim 830°C$, and the Neél temperature corresponding to the onset of antiferromagnetism is $\sim 370°C$, which means that magnetoelectric coupling can be observed at room temperature. However this is not the linear magnetoelectric effect as described above, as in fact the antiferromagnetic state has a long ranged spin cycloidal component, rather than each spin being strictly anti-parallel to each other. This means that the spontaneous polarization conferred by the magnetic moments averages to zero across the cycloid. Nevertheless, multiferroicity is still observed due to a quadratic component to the magnetoelectric coupling. The polarization causes a breaking in symmetry and induces a slight canting of the spins *via* the Dzyaloshinskii-Moriya interaction:

$$\mathcal{H} = \sum D_{ij} \cdot S_i \times S_j$$

The cross product describes this canting.

In common with other ferroelectric materials, bismuth ferrite contains ferroelectric domains. A ferroelectric domain is a microscopic area of the material where the polarisation of all the molecules lies in a similar direction. Defects in the material result in domain walls being formed, either side of which lie different domains; the polarisation of these domains tend to lie in different directions. The domain walls can be defined in terms of the difference in direction of the respective polarisations of the domains. For bismuth ferrite, these angles are: 71°, 90°, 109° and 180°. Previous studies by Zavaliche [2] and

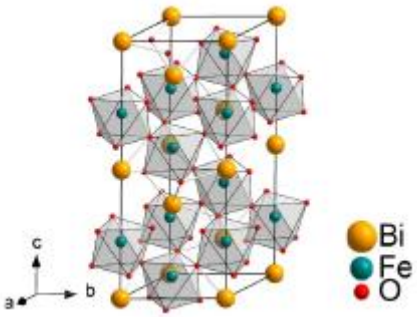

Figure 1: Structure of bismuth ferrite as depicted by Lebeugle [4]

Chu [3] have shown the presence of these domains on thin films using AFM and PFM measurements respectively. This paper will detail the use of coherent X-ray radiation in imaging these domains.

There are two requirements in obtaining coherent X-rays: a large brilliance and a small source size. Synchrotron sources (in particular third-generation sources) satisfy both of these requirements. All synchrotron radiation sources emit some degree of coherent radiation. The extent of this radiation can be defined in terms of the coherence volume, which can be decomposed into the longitudinal and transverse coherence lengths:

$$l_T = \frac{\lambda D}{d},$$

where D is the distance of the sample from the source, and d is the size of the source:

$$l_L = \frac{\lambda^2}{\Delta\lambda}.$$

The transverse coherence volume for most beamlines is of the order of 10–20μm, which is the main consideration here. [5] The coherence of a beam can be increased *via* the use of undulators, which reduce the size of the source and help to monochromatize the beam, pinholes and increasing the distance between the source and the detector. The mounting of a detector arm onto the diffractometer aids in increasing coherence, a useful addition since the distance between source and sample is fixed for each beamline in its construction. Incoherent X-ray sources (such as those typically found in a laboratory) produce a characteristic diffraction pattern when a crystalline source is imaged, a Laue pattern. However when a coherent source is used, interference fringes are observed, a so-called speckle pattern. This speckle pattern contains detailed information about the structure of a material. This speckle pattern is observed when using any coherent optical source (for example a laser) but X-rays provide the benefit of being more sensitive at much smaller length scales. Various techniques exist for reconstructing the structure of a crystal from the X-ray speckle pattern, in particular ptychography, which utilises an algorithm to overcome the so-called 'phase problem' of crystallography. [6] [7] [8]

2 Experimental methods

Measurements were carried out on a single crystal of $BiFeO_3$ which had previously been used for other experiments. X-ray measurements were carried out at beamline I16 at Diamond Light Source. This beamline was designed with materials and magnetism research in mind, and was the ideal one to use for our research. The sample at I16 is 50m from the source. The synchrotron radiation was collimated using an undulator, focused in the optics hutch and monochromated using the (006) plane of graphite to obtain the X-ray beam (7.835 keV, 5 $\times$ 2.5 mm beamsize). This beam was passed through a 20μm pinhole to eliminate the majority of the flux and ensure a coherent beam, diffracted by the sample which was mounted on a six-circle diffractometer and the outgoing radiation collected by a Princeton Instruments CCD (pixel size 11μm) mounted on a 3m long detector arm. This CCD was used as the small pixel size would enable very fine detail to be seen, despite the smaller resolution conferred by this camera with

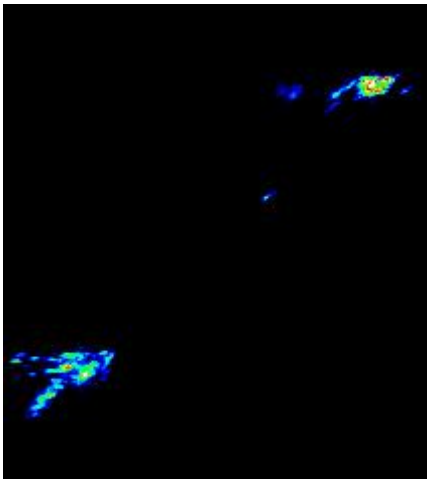

Figure 2: Image captured in WinView by the CCD which clearly shows two peaks, the upper right and lower left peaks. On the lower left peak interference fringes (Fraunhofer) occur as a result of the coherent X-ray radiation.

respect to others that were available. The diffractometer was fitted to a Princeton Instruments piezo stage (0–10V) for additional scanning capabilities in the x and y directions.

In order to image the ferroelectric domains, a darkfield image was taken of one of the Bragg peaks. Next the sample was moved stepwise by the piezo stage in both the x and y directions in the manner of a raster scan, so that a series of images were built up by the CCD. These images were analysed using WinView (Fig. 2), and regions of interest corresponding to areas of increased intensity of *ca.* 90×90 pixels picked out on the CCD images. For each frame, the integrated intensity of the whole CCD was exported as a single number. This series of numbers was rearranged into a matrix corresponding to the grid over which the raster scan was performed, and contour plots produced in Origin. In addition the peak width as a function of raster scan was also determined. This was performed by taking x and y-cross sections of peaks using WinView, which gave the intensity as a function of each pixel per frame. This naturally gave a large number of data points, so Octave (an open-source relative of MATLAB) was used to manipulate it. The number of pixels with intensity non-zero were determined per frame, and then a matrix constructed such that the grid was formed. Contour plots of these cross sections were also made in Origin.

3 Results

Two peaks were present on the detector during our scans in the eta circle. At $\eta = 16.36°$ both were visible on the detector at the same time. These will henceforth be referred to as the lower left (LL) and upper right (UR) peaks, which is due to their position on the detector. What is noticeable about these contour plots is that there appears to be a degree of stripe-like characteristics which extend from the top left to the bottom right corners of each image, that is 45° to the $p_x p_y$ plane, where p_x is the horizontal movement of the piezo stage and p_y is the vertical in the laboratory frame. This is more evident in the images from the lower left peak, however it can still be seen in upper right peak plots. These are believed to be the ferroelectric domains, and previous studies have detailed that along the [111] set of directions they appear distinctly striped. "Reference" In-plane PFM phase images by Lebeugle [4] of a single crystal of $BiFeO_3$ also exhibit the fractal behaviour of the domains.

In reciprocal space, the peaks that were observed correspond to the [0 $\bar{1}$ 1] direction as determined by the UB matrix which was calculated empirically. However what is required is the direction of the domains in real space.

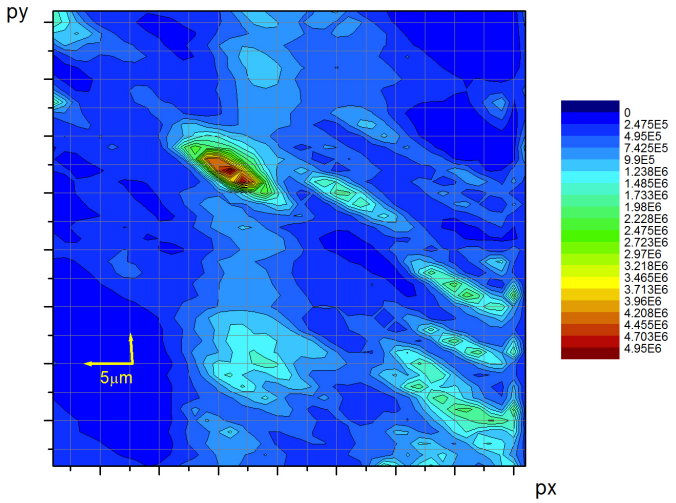

Figure 3: Contour plot showing the integrated intensity of the lower left peak as a function of raster scan. px and py range from 1-5V. Note the stripe-like features descending towards the bottom-right corner.

The stripes observed on the contour plots lie in a plane containing the peak in reciprocal space, since the plots relate to the intensity of the peak as a function of the raster scan. A peak in reciprocal space corresponds to an (hkl) plane in real space, so if the reciprocal lattice of $BiFeO_3$ can be determined, then the [0 $\bar{1}$ 1] peak can be converted into a Miller plane, and hence the stripe direction determined.

The [0 $\bar{1}$ 1] peak in reciprocal space would transform into the [0 $\bar{1}$ 1] plane in real space, if a pseudo-cubic lattice is assumed. The direction that lies in the plane, but at 45° to the (0 $\bar{1}$ 1) direction is the ($\bar{1}$ $\bar{1}$ 1) direction. This is a member of {111}, and hence agrees with the previously obtained data. These domains correspond to the 109° domain walls, as they lie along the body-diagonals of a pseudo-cubic lattice. Lubk [9] has performed first principles studies of the ferroelectric domain walls and found that the 109° domain wall also has the lowest energy, although their study used the (0 0 1) plane for the domain wall, with the polarisation changing from the [1 1 1] to the [$\bar{1}$ $\bar{1}$ 1] direction either side of the domain wall.

We have analysed coherent X-ray diffraction patterns of a single crystal of bismuth ferrite and determined the intrinsic ferroelectric domain wall structure, finding that the results agree with previous publications. Future possible areas for research include applying an electric field to the crystal of $BiFeO_3$ and imaging domain wall movement, including time-dependence.

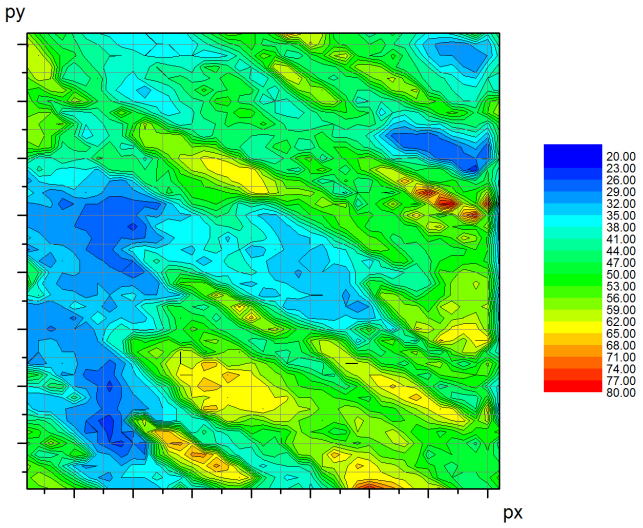

Figure 4: This figure shows the cross section of the peak as a function of raster scan, which gives further details into the domain walls. The x-cross section (top) shows the stripe-like features observed in other plots, whereas the y-cross section (bottom) is less defined.

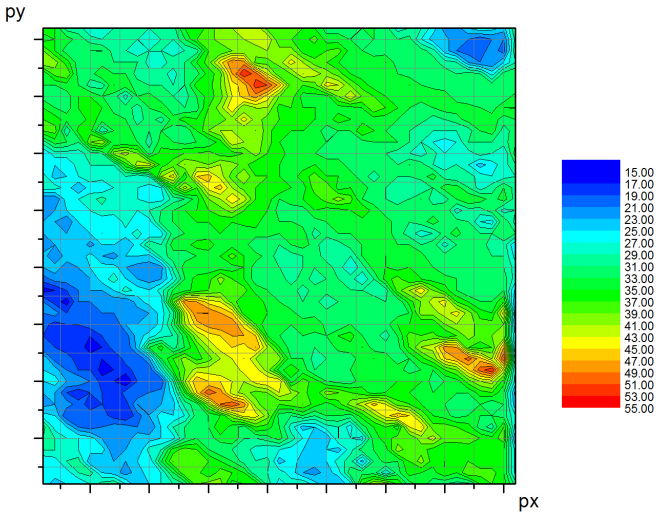

Appendix

The diffractometer used on beamline I16 is a six-circle diffractometer, which has six rotational degrees of freedom: ϕ, η, χ, δ, γ and μ. These correspond to various rotation matrices, which are transformations of the Cartesian axes. In this experiment μ was set to zero, meaning that in effect it was a five-circle setup.

References

[1] G. Catalan and J. F. Scott, *Adv. Mater.* **21**, 2463 (2009).

[2] F. Zavaliche, S. Y. Yang, T. Zhao, Y. H. Chu, M. P. Cruz, C. B. Eom and R. Ramesh, *Phase Transitions* **79**, 991 (2006).

[3] Y. H. Chu, T. Zhao, M. P. Cruz, Q. Zhan, P. L. Yang, L. W. Martin, M. Huijben, C. H. Yang, F. Zavaliche, H. Zheng and R. Ramesh, *Appl. Phys. Lett.* **90**, 252906 (2007).

[4] D. Lebeugle, D. Colson, A. Forget, M. Viret, P. Bonville, J. F. Marucco and S. Fusil, *Phys. Rev. B* **76**, 024116 (2007).

[5] J. Als-Nielsen and D. McMorrow, Elements of X-ray Physics, Wiley (Chichester), 2011.

[6] A. Szöke, *Acta Cryst. A* **57**, 586 (2001).

[7] J. M. Rodenburg, *Advances in Imaging and Electron Physics* **150**, 87 (2008).

[8] X. Huang, R. Harder, G. Xiong, X. Shi and I. Robinson, *Phys. Rev. B* **83**, 224109 (2011).

[9] Axel Lubk, S. Gemming and N. A. Spaldin, *Phys. Rev. B* **80**, 104110 (2009).